The role of storm-track dynamics in the intraseasonal variability of the winter ENSO teleconnection to the North Atlantic

Received: 18 August 2023 | Revised: 22 December 2023 | Accepted: 12 February 2024

DOI: 10.1002/qj.4691

Quarterly Journal of the Royal Meteorological Society RMetS

RESEARCH ARTICLE

The role of storm-track dynamics in the intraseasonal variability of the winter ENSO teleconnection to the North Atlantic

Christopher H. O'Reilly[1] | **Marie Drouard**[2] | **Blanca Ayarzagüena**[3] | **Maarten H. P. Ambaum**[1] | **John Methven**[1]

[1]Department of Meteorology, University of Reading, Reading, UK

[2]Instituto de Geociencias, CSIC-UCM, Madrid, Spain

[3]Departamento de Física de la Tierra y Astrofísica, Universidad Complutense de Madrid, Madrid, Spain

Correspondence
Christopher H. O'Reilly, Department of Meteorology, University of Reading, Reading, RG6 6BB, UK.
Email: c.h.oreilly@reading.ac.uk

Funding information
Royal Society, Grant/Award Number: URF\R1\20123

Abstract

The response of the North Atlantic large-scale circulation to El Niño–Southern Oscillation (ENSO) exhibits distinct differences between early (November–December) and late (January–February) winter. However, the reasons for this are unclear, particularly regarding the early winter response. Here we examine the role of storm-track dynamics in influencing the intraseasonal variability of the ENSO teleconnection to the North Atlantic. During late winter there a broad weakening of the eddy heat flux upstream of the North Atlantic storm track during the El Niño phase, which is associated with a broad southward jet shift across North America and the North Atlantic. The late winter response is reinforced by synoptic eddies through enhanced cyclonic wave breaking, consistent with previous studies. However, a stronger teleconnection occurs during early winter. There are modest changes in the North Atlantic eddy heat flux, but strong changes in the upper-level storm track associated with ENSO, with increased anticyclonic wave breaking during El Niño reinforcing the jet across the central North Atlantic. During early winter there are less frequent northern eddy-driven jet occurrences in El Niño years and more frequent northern eddy-driven jet occurrences in La Niña years. These poleward North Atlantic jet excursions typically follow peaks in the eddy heat flux; however, in El Niño years this relationship breaks down and the jet does not transition to the northern position as frequently, despite no clear changes in the upstream eddy heat flux. Composite analysis reveals that precursor storm-track anomalies upstream over the eastern North Pacific/North America are important in suppressing the poleward jet excursions. These precursors map onto the seasonal mean North Pacific storm-track anomalies during El Niño. Measured across all years, there is a clear relationship between the mean early winter eastern North Pacific storm-track activity and eastern North Atlantic eddy-driven jet, which can explain the early winter ENSO teleconnection to the North Atlantic.

KEYWORDS

dynamic processes, seasonal, scale, dynamics, ENSO, midlatitude, NAO

1 | INTRODUCTION

The El Niño–Southern Oscillation (ENSO) phenomenon is characterised by coupled ocean–atmosphere variability in the Tropical Pacific but has remote influences across the globe, through atmospheric teleconnections (e.g., Horel & Wallace, 1981; Trenberth et al., 1998; Wallace & Gutzler, 1981). The shifting patterns of tropical convection associated with ENSO influence the upper-level jet streams and associated storm tracks, which has a significant influence on seasonal climate variability in many continental regions in the extratropics (e.g., Trenberth, 2020). In the Northern Hemisphere, the strongest extratropical influence of ENSO is seen in the North Pacific sector, where the North Pacific jet shifts south and strengthens further downstream, significantly influencing the climate of North America (e.g., Cook et al., 2007; Seager, Naik, et al., 2010; Seager, Kushnir, et al., 2010).

ENSO has also been shown to influence the large-scale circulation in the extratropical North Atlantic region significantly, with an associated impact on the seasonal climate conditions of the surrounding continental regions of Europe and North America (e.g., Brönnimann et al., 2007; Taschetto et al., 2020). Moreover, the ENSO teleconnection to the North Atlantic provides an important source of predictability in wintertime seasonal forecasts (e.g., Dunstone et al., 2016; O'Reilly et al., 2020; O'Reilly, Heatley, et al., 2017; Scaife et al., 2014; Smith et al., 2012; Thornton et al., 2023).

Given the importance of ENSO as a source of seasonal predictability, there have been many studies into the mechanisms governing the teleconnection to the extratropical North Atlantic. Previous studies have highlighted the significant influence of ENSO on the North Atlantic Oscillation (NAO: e.g., Brönnimann et al., 2007; Pozo-Vázquez et al., 2005a,b), which is the dominant mode of large-scale circulation variability in the North Atlantic sector and is characterised by stronger/weaker meridional sea-level pressure gradient over the entire basin (e.g., Hurrell et al., 2003). Previous studies have shown that the link between ENSO and the NAO is particularly strong in late winter (i.e., January–March), with negative NAO conditions more likely during El Niño winters and positive NAO conditions more likely during La Niña winters (e.g., Brönnimann et al., 2007; Drouard et al., 2015; Li & Lau, 2012; Toniazzo & Scaife, 2006).

The mechanisms linking ENSO to the phase of the late winter (January–February) NAO in the literature can broadly be grouped into stratospheric and tropospheric pathways. The stratospheric pathway is characterised by changes in the strength of the upward-propagating planetary waves; this anomalous propagation acts to weaken the stratospheric polar vortex in El Niño winters and strengthen the stratospheric polar vortex in La Niña winters (e.g., Domeisen et al., 2019). These stratospheric signals subsequently exhibit a downwards impact on the troposphere, ultimately influencing the likely phase of the NAO (e.g., Butler et al., 2014; Hardiman et al., 2019; Ineson & Scaife, 2009).

The tropospheric pathway is characterised by changes in the Pacific jet stream and the propagation of eddy energy into the North Atlantic sector. The North Pacific jet strengthens and extends zonally across the North Pacific due to eddy momentum flux feedbacks during El Niño winters (e.g., Seager, Naik, et al., 2010). There is a subsequent influence on the eddy propagation into the North Atlantic sector (e.g., Jiménez-Esteve & Domeisen, 2020), with the associated anomalous eddy momentum fluxes acting to favour the particular phases of the NAO (Drouard et al., 2015; Li & Lau, 2012).

Whilst most of the literature has focused on the ENSO teleconnection to the North Atlantic in the late winter, recent studies have emphasised the intraseasonal variability of the teleconnection. In the early winter (November–December), the teleconnection is quite different from that in the late winter, with the associated sea-level pressure anomalies closely resembling the "East Atlantic" pattern (EA) rather than the NAO (Ayarzagüena et al., 2018; Geng et al., 2023; King et al., 2018; King et al., 2023; Moron & Gouirand, 2003), as also shown here in Figure 1a; in addition, some studies have highlighted the possible role of the tropical Indian Ocean in modifying the ENSO teleconnection to the North Atlantic in early winter (Abid et al., 2021, 2023). Previous studies have demonstrated that free-running coupled climate models struggle to reproduce the early-season teleconnection to the North Atlantic (Ayarzagüena et al., 2018; Molteni, 2020). Some seasonal forecasting systems seem to resemble the observed teleconnection more closely in early winter, but the response is inconsistent and weaker than that seen in observations (Ayarzagüena et al., 2018; Molteni & Brookshaw, 2023; Thornton et al., 2023). In order to identify the causes for such apparent modelling deficiencies, it is important to first develop understanding of the mechanisms driving the early winter teleconnection. To date, however, this has received relatively little attention in the literature; investigating the mechanisms underlying the early winter teleconnection to the North Atlantic is a key focus of this study.

To understand the response of the extratropical North Atlantic large-scale circulation to ENSO, in the analysis that follows we explore changes in the regime behaviour and the associated storm track lifecycle in the North Atlantic. On subseasonal timescales, the variability of the wintertime North Atlantic eddy-driven zonal jet

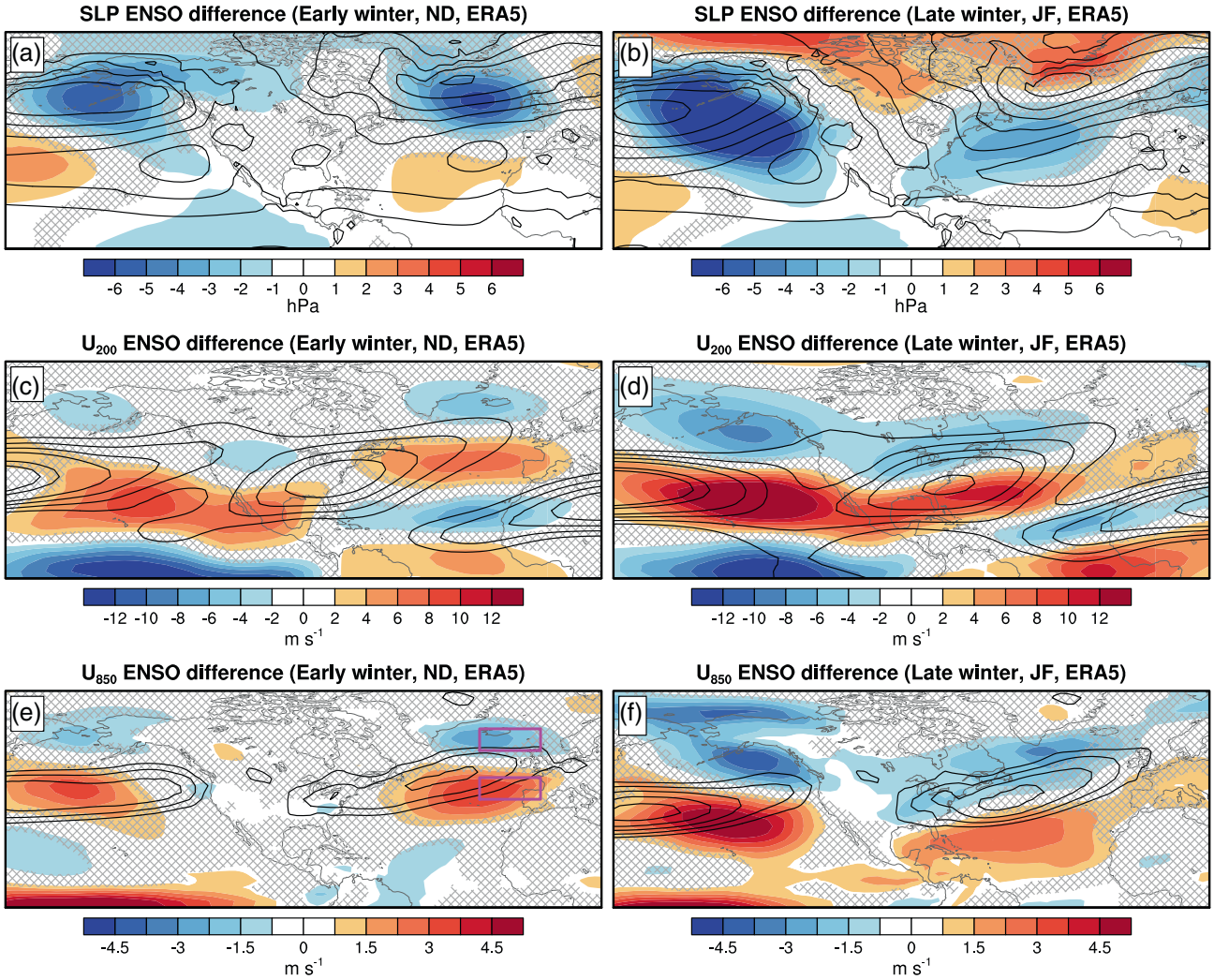

FIGURE 1 Difference between El Niño and La Niña phases in early winter, ND, and late winter, JF, for (a,b) SLP, (c,d) u at 200 hPa, and (e,f) u at 850 hPa. The climatologies (1950–2022) of each field for the different periods are contoured, with contour intervals (a,b) 4 hPa, (c,d) 5 m·s^{-1} from 20 m·s^{-1}, and (e,f) 1.5 m·s^{-1} from 6 m·s^{-1}. Hatching indicates regions where the difference has p-values greater than 0.1, based on a Monte Carlo resampling.

(i.e., in the lower troposphere) exhibits a trimodal latitude distribution that sets it apart from other extra-tropical storm-track regions and seasons (Woollings et al., 2010). These regimes are robust across different observational datasets and periods and correspond closely to circulation regimes found through cluster analysis of daily geopotential height anomalies over the North Atlantic sector (e.g., Vautard, 1990). Novak et al. (2015) showed that some of the more common transitions are linked to the lifecycle-type behaviour of the North Atlantic storm track (Ambaum & Novak, 2014), with peaks in storm-track activity (i.e., eddy heat flux) in the western North Atlantic linked with poleward displacements of the eddy-driven jet, and subsequent weaker periods associated with a more southern jet position. Moreover, sensitivity experiments demonstrate that higher upstream heat fluxes have been shown to result in a higher frequency of poleward displacements of the eddy-driven jet (O'Reilly, Minobe, et al., 2017).

In this study, we examine the role of storm-track dynamics in governing the mean seasonal response of the North Atlantic large-scale circulation to ENSO using reanalysis data. In particular we focus on the regime behaviour of the eddy-driven jet and how this relates to the storm-track activity; we find that the observed seasonal mean responses in early and late winter can be interpreted as changes in occurrence of the different eddy-driven jet latitude regimes. We show that there are changes in the relationship between the storm-track activity and the eddy-driven jet that are clearly linked to the upstream influence of the North Pacific jet—but there are distinct differences between early and late winter that are

important in generating the intraseasonal variability of the ENSO teleconnection.

2 | DATASETS AND METHODS

2.1 | Reanalysis data and storm-track diagnostics

We analyse data from the ERA5 reanalysis dataset (Hersbach et al., 2020) over the period 1950–2022, which includes a total of 72 winters. The daily mean data were regridded to $1\circ \times 1\circ$ horizontal resolution prior to the analysis. To examine the role of storm-track activity and associated eddy–mean-flow interactions, we analyse high-pass eddy variables. These eddies were calculated by taking daily mean variables and running them through an eight-day high-pass filter, specifically a 31-point Lanczos filter (Duchon, 1979). In the analysis that follows we examine several storm-track diagnostics.

- *Meridional eddy heat flux*: defined as the poleward transport of heat at 850 hPa in the lower troposphere by synoptic (high-pass filtered) eddies, $\overline{v'T'}$. The eddy heat flux is an important measure of baroclinic wave growth and reflects the tendency of baroclinic waves to transport heat polewards over their lifecycle, generating eddy kinetic energy at the expense of available potential energy.
- *Eddy kinetic energy (EKE)*: defined here as a measure of the EKE of synoptic (high-pass filtered) eddies at 200 hPa in the upper troposphere, $K = \frac{1}{2}(\overline{u'^2 + v'^2})$.
- *Eddy total energy flux (TEF)*: is a measure of the flux of energy associated with synoptic eddies, including the eddy available potential energy and eddy kinetic energy, defined as $TEF = \mathbf{v}(K + P) + \mathbf{v}'\phi'$. The first term represents the advection of eddy kinetic energy (K, as above) and eddy available potential energy, P (following, e.g., Drouard et al. (2015)). The eddy available potential energy is defined as $P = \left[h^2/(2s^2)\right]\theta'^2$, where θ' is the high-pass filtered potential temperature and the parameters $s^2 = -h(\partial\theta_R/\partial p)$ and $h = (R/p)(p/p_s)^{R/C_p}$ are constants that depend only on the pressure level (θ_R is a reference potential temperature; R is the gas constant; p_s is the reference pressure level; C_p is the specific heat capacity). The second term represents the ageostrophic geopotential flux of synoptic eddies, where $\mathbf{v}_a$ is the horizontal ageostrophic velocity and ϕ is the geopotential; this term has been linked to downstream development of baroclinic waves (e.g., Orlanski & Chang, 1993). Together, these provide a measure of the total energy propagation of synoptic eddies. In the analysis that follows we evaluate the TEF at 200 hPa in the upper troposphere, with a particular focus on the zonal component.
- ***E** vectors*: here we analyse the horizontal components, $\mathbf{E} = [E_x, E_y] = [(v'^2 - u'^2)/2, -u'v']$, which provide a measure of the shape and tilt of the synoptic eddies and can be used to estimate the feedback of the eddies onto the mean flow (Hoskins et al., 1983). We examine the **E** vector at 200 hPa in the upper troposphere. The meridional component of the **E** vector is an important measure of the direction of synoptic wave breaking, with poleward vectors indicating cyclonic wave breaking and equatorward vectors indicating anticyclonic wave breaking. The tendency of the synoptic eddies in forcing the low-frequency zonal flow, through momentum flux convergence, can be estimated by taking the divergence of the **E** vector (e.g., Trenberth, 1986).

2.2 | North Atlantic eddy-driven jet diagnostic

In addition to the storm-track diagnostics we also evaluate the behaviour of the North Atlantic eddy-driven jet. We broadly follow the approach of (Woollings et al., 2010) to identify the location of the eddy-driven jet in the North Atlantic. The daily mean zonal wind at 850 hPa in the lower troposphere is averaged over the region 0–60°W, retaining values between 15 and 75°N. The zonal mean zonal wind is then low-pass filtered using a 10-day Lanczos filter to identify changes in the jet on timescales longer than those of individual synoptic systems. The maximum wind speed on each day is then identified as the latitude of the North Atlantic eddy-driven jet. The daily jet latitudes are then used to calculate jet latitude distributions using a kernel estimate with standard smoothing parameter $h = 1.06\sigma n^{-1/5}$, where σ is the standard deviation and n is the sample size (Silverman, 1981). In the pdfs presented below, we use the same h calculated from all years for the La Niña and El Niño subsets to aid comparison with the climatological distribution.

2.3 | Blocking-event diagnostic

We analyse the changes in blocking frequency by using a two-dimensional large-scale wave-breaking index, commonly used to identify blocking events in the literature (e.g., Woollings et al., 2008). Here we follow the methodology of (Masato et al., 2013). The index uses daily $Z500$ data and identifies meridional reversals of the normal equator-to-pole gradient, over regions of 15° to the north

and south of each point in the northern midlatitudes. Events must span at least 15° in longitude and must persist for at least five days to be identified as blocking events according to this diagnostic.

2.4 | ENSO definitions

To define ENSO years we follow the "Oceanic Niño Index" (ONI) methodology of National Oceanic and Atmospheric Administration (NOAA), applied to the Hadley Centre Sea Ice and Sea Surface Temperature (HadISST) dataset (Rayner et al., 2003). The ONI methodology used three-month averages of SSTs averaged over the Niño 3.4 index region (170°W–120°W, 5°S–5°S). Anomalies with a magnitude greater than 0.5° K relative to a moving 30-year averaged climatology are defined as ENSO winters. The anomaly must remain over the threshold for four consecutive three-month seasons, one of which must be DJF, to satisfy the criteria of being an ENSO winter. A total of 19 El Niño winters and 18 La Niña winters are identified in the 72 winters over the period of this study.

2.5 | Significance testing

To provide a measure of the statistical significance for the composite ENSO differences presented below, we compare the observed composite differences with distributions of randomly sampled composites. Specifically, two composites with the equivalent number of years are resampled at random from the entire dataset to produce random composites and the difference of these is recorded. This process is repeated 10 000 times and the resulting distribution is used to estimate *p*-values, which provide some context to the magnitude of the observed anomalies. Where the observed ENSO composite differences are large compared with the random distribution, this provides positive evidence that ENSO plays a role in governing the differing circulation responses (Ambaum, 2010).

3 | RESULTS

3.1 | Intraseasonal variability in the large-scale circulation and storm-track response to ENSO

We begin our analysis by examining the extratropical ENSO teleconnection over the North Atlantic sector (and extended over the western North Pacific) in terms of early/late winter mean large-scale atmospheric circulation. Figure 1 shows the composite ENSO difference—defined here as the composite El Niño winter average minus the composite La Niña winter average—for sea-level pressure (SLP), zonal wind in the upper troposphere (at 200 hPa, $U200$) and zonal wind in the lower troposphere (at 850 hPa, $U850$). We focus our analysis on early (November–December) and late (January–February) winter periods, following Ayarzagüena et al. (2018). Analysis of individual months from October–March (Figure S1) reveals that the clearest ENSO influence over the North Atlantic is in the November–February period and confirms that there is a distinct shift between the early (ND) and late (JF) winter periods, as highlighted in previous studies.

The large-scale circulation response in SLP over the North Atlantic (Figure 1a,b) is substantially different in the early winter (ND) compared with late winter (JF). In early winter, the SLP difference has a strong low in midlatitudes mapping approximately onto the "East Atlantic Pattern", whereas in late winter the SLP difference resembles the negative phase of the NAO pattern. This difference was highlighted by Moron and Gouirand (2003), Ayarzagüena et al. (2018), and King et al. (2018). It is of interest to go beyond large-scale SLP anomalies and analyse the changes in the North Atlantic jet. The equivalent zonal wind differences (Figure 1c–f) show that in the early winter period the jet response to ENSO in the North Atlantic is generally found further downstream towards Europe and is strongest in the midlatitudes, where the jet stream is further south during El Niño winters. In contrast, the late winter teleconnection has stronger changes further south in the Atlantic, with the zonal wind anomalies spanning most of the North Atlantic basin and not just confined to the midlatitudes as in early winter.

To understand further the processes governing the variations between the early and late winter ENSO response in the North Atlantic, we examine differences in seasonal mean storm-track measures, shown in Figure 2. We first examine differences in the meridional eddy heat flux, $\overline{v'T'}$, at 850 hPa (Figure 2a,b). In the early winter there is relatively little difference in the meridional eddy heat flux over the peak climatological storm-track region (shown in contours), with a slight meridional shift reflecting the changes in the mean jet (i.e., Figure 1c,e). The lack of clear changes in the meridional eddy heat flux over North America and the peak climatological storm-track region during the early winter period is consistent with the fairly modest changes in the upper-tropospheric jet around the west coast of North America (i.e., Figure 1c). In contrast, in the late winter there is a broad weakening in the meridional eddy heat flux over North America and a larger-scale southward shift over the North Atlantic basin, which is consistent with the lifecycle behaviour shown by Novak et al. (2015). The broad weakening over North America and the western North Atlantic in the

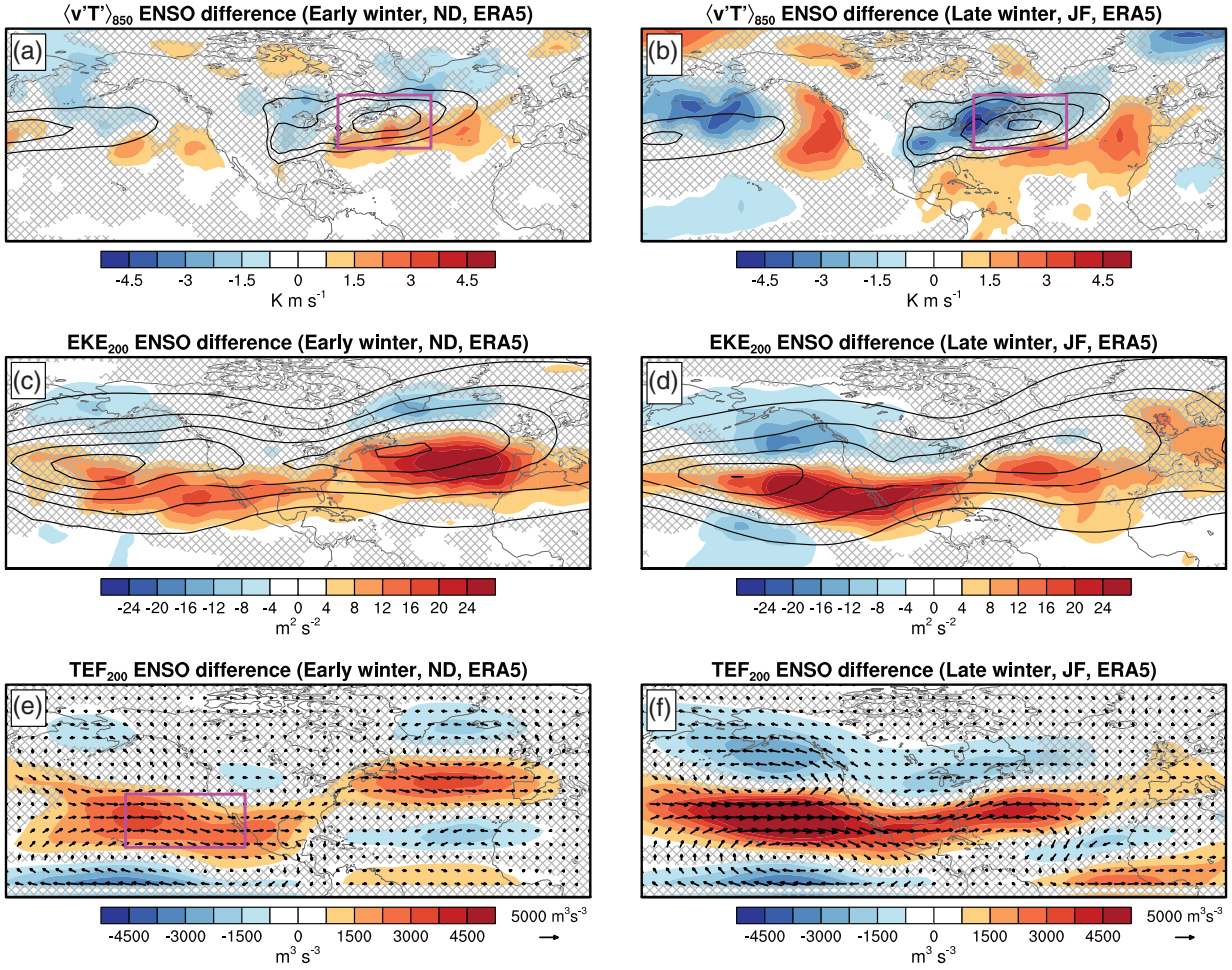

FIGURE 2 Difference between El Niño and La Niña phases in early winter, ND, and late winter, JF, for (a,b) eddy heat flux, $v'T'$, at 850 hPa, (c,d) EKE at 200 hPa, and (e,f) zonal component of TEF at 200 hPa. For (a–d), the climatologies (1950–2022) of each field for the different periods are contoured, with contour intervals (a,b) 4 K·m·s^{-1} from 8 K·m·s^{-1} and (c,d) 20 m^2·s^{-2}. The vectors in (e,f) show the TEF difference. Hatching indicates regions where the difference (shaded) has p-values greater than 0.1, based on a Monte Carlo resampling.

late winter largely follows the large-scale shift of the upper-tropospheric zonal wind between ENSO phases in the late winter (i.e., Figure 1d), which is associated with a change in large-scale wind shear and associated baroclinicity (as measured by the Eady growth rate, shown in Figure S2).

We now examine the EKE and TEF at 200 hPa in the upper troposphere in the different phases of ENSO (Figure 2c–f). Both of these storm-track diagnostics show a consistent southward shift of the storm track and a slight strengthening during El Niño winters compared with La Niña winters. This is broadly seen in both early (ND) and late (JF) winter periods spanning the eastern North Pacific and across the North Atlantic. One prominent feature, however, is that the EKE difference in the North Atlantic is stronger in the early winter than the late winter, despite the changes upstream over the North Pacific/America region being weaker.

The zonal component of the TEF differences (Figure 2e,f) largely resemble the patterns of upper-tropospheric zonal wind differences between the ENSO phases (i.e., Figure 1c,d), with the late winter differences showing a strong zonal downstream flux of eddy energy from the North Pacific across Mexico and into the North Atlantic (Figure 2f). The strong downstream TEF across this region was found to be an important tropospheric pathway for the ENSO influence on the North Atlantic in previous observational and idealised studies (Jiménez-Esteve & Domeisen, 2018, 2020). The early-winter TEF differences, in contrast, show less clear changes in the zonal downstream flux of eddy energy from the North Pacific, with a less clear connection around the west coast of North America. This is particularly noteworthy because the differences in the North Atlantic sector show a more statistically significant response than in the late winter period, indicating that the mechanisms

through which changes over the North Pacific influence the North Atlantic are different in the early winter.

To investigate how these storm-track changes are influencing the large-scale circulation differences seen over the North Atlantic between ENSO phases, we now examine the horizontal **E**-vector composites, shown in Figure 3a–f. As outlined in Figure 2b, the **E** vectors are a useful diagnostic of the zonal momentum fluxes by synoptic eddies, with divergence of the **E** vector indicating where the eddies act to force the zonal flow. During El Niño in the early winter, there are stronger equatorward **E** vectors over the eastern North Atlantic, indicative of stronger anticyclonic wave breaking, with the associated momentum fluxes acting to drive the zonal jet in a more zonal orientation and in a more southern position south than during La Niña. The divergence of the **E** vectors is fairly noisy, but the difference (shown in Figure 3e) nonetheless highlights the action of the eddies in driving the zonal wind differences over the eastern North Atlantic.

The **E**-vector composites in the late winter period exhibit a substantially more poleward orientation during El Niño, in contrast to the early winter period (Figure 3b,d). The region of anomalously poleward **E** vectors—and associated cyclonic wave breaking—spans from North America all the way across the North Atlantic (Figure 3f), with the divergence demonstrating that the eddies are acting to force the jet further south during El Niño—and substantially further south than during the early winter (cf. Figure 1e,f). Overall, this beahviour is consistent with previous studies that have shown increased cyclonic wave breaking during the late winter period in El Niño years compared with La Niña years (Drouard et al., 2015; Li & Lau, 2012).

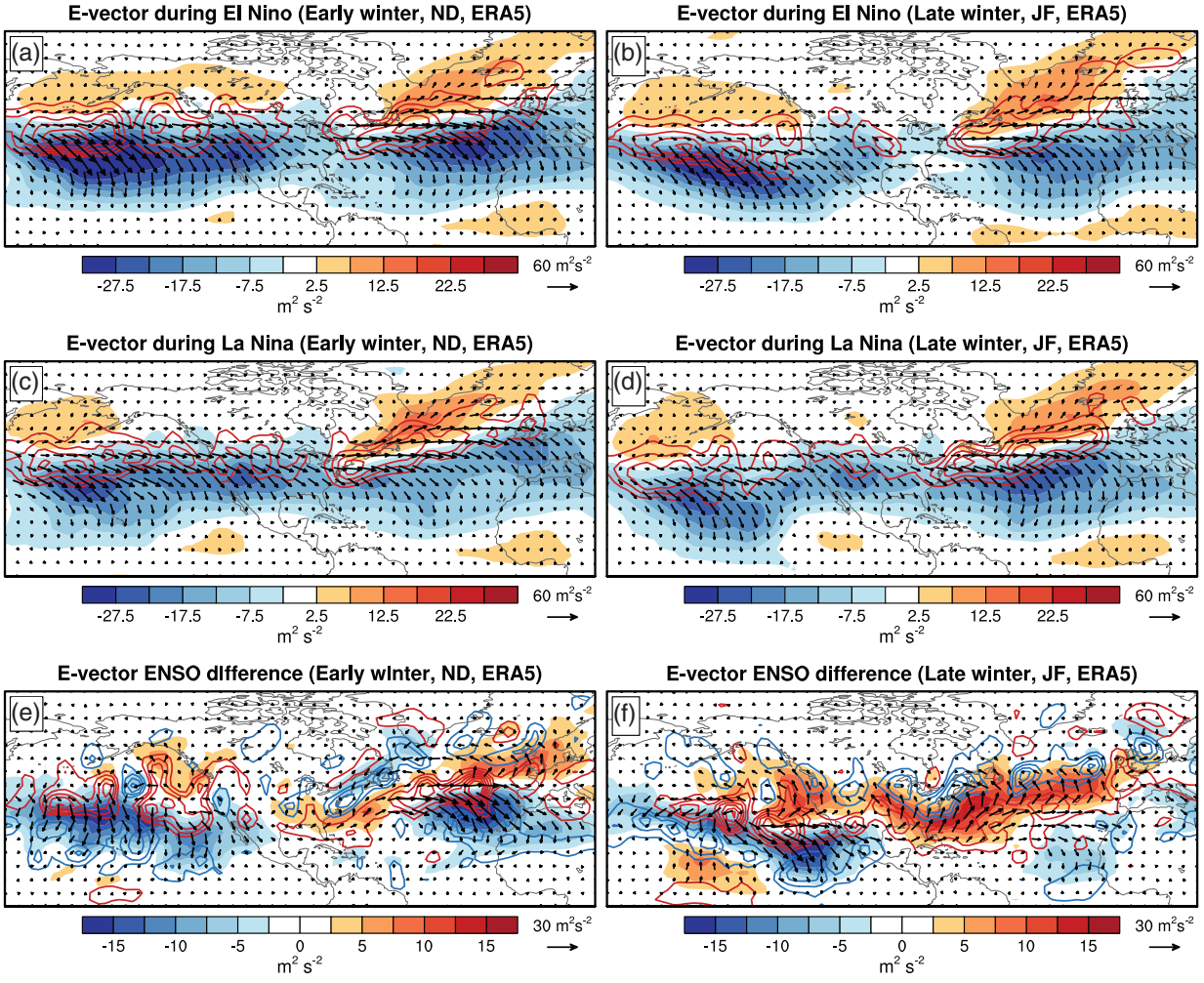

FIGURE 3 (a,b) El Niño and (c,d) La Niña composites and (e,f) difference in early winter, ND, and late winter, JF, for E_y at 200 hPa. For (a–d), the vectors show the full **E** vector at 200 hPa and the divergence of the **E** vector is shown in contours every 0.5 $m^2 \cdot s^{-2} \cdot day^{-1}$ from 0.5 $m^2 \cdot s^{-2} \cdot day^{-1}$. For (e,f), the vectors show the **E**-vector difference at 200 hPa and the difference of the **E**-vector divergence is shown in contours every 0.3 $m^2 \cdot s^{-2} \cdot day^{-1}$ (with the zero contour omitted), with negative values in blue and positive values in red. A separate plot of the **E**-vector divergence is included in the Supplementary Material, Figure S3.

The study by Ayarzagüena et al. (2018) found that upper-level Rossby-wave source anomalies over eastern North America were significantly different between ENSO phases and discussed the possibility that this could drive a stationary Rossby-wave response downstream. The Rossby-wave source is roughly proportional to the meridional gradient of the **E**-vector divergence (e.g., Hoskins et al., 1983), so it is clear we are picking up similar signals in the **E**-vector diagnostics shown in Figure 3e,f. In the following sections, we show that the season mean response is perhaps better understood through systematic changes in the subseasonal circulation rather than a stationary Rossby-wave response.

In this section we have revisited the contrasting North Atlantic large-scale circulation anomalies in early and late winter associated with ENSO. There are distinct differences in the response of the North Atlantic jet between early and late winter, which show a clear barotropic structure (i.e., Figure 1c–f). Examining the ENSO differences in terms of some storm-track diagnostics reveals that the average responses in early and late winter have some clear differences. In late winter there is a broad weakening of the eddy heat flux upstream of the North Atlantic storm track during the El Niño phase, which is associated with a broad southward shift of the jet stream across North America and the North Atlantic. As highlighted in previous studies, this late winter response is reinforced by eddies through enhanced cyclonic wave breaking. In contrast, during early winter there are only modest changes in the eddy heat flux over the North Atlantic but there are strong changes in the upper-level storm track associated with ENSO, with an increase in anticyclonic wave breaking during El Niño and the eddies acting to reinforce the jet across the central part of the North Atlantic. Overall, these results indicate that there are distinct differences in the mechanisms by which the upstream North Pacific influences the North Atlantic during early and late winter, and that these are important in contributing to the mean ENSO response.

3.2 | The behaviour of the North Atlantic eddy-driven jet during different phases of ENSO

In the previous section we analysed the mean ENSO differences in early and late winter, highlighting the different storm-track dynamics between the two periods. However, analysing these seasonal mean responses only allows us to identify common relationships between the large-scale circulation response to ENSO and associated storm-track dynamics. To understand better how the dynamics of the North Atlantic circulation change during ENSO phases, and the role of the storm track in governing this, it is useful for us to examine the subseasonal variability of the North Atlantic eddy-driven jet and the associated storm-track dynamics, as we will here and in the following section.

Distributions of the subseasonal variability of the North Atlantic eddy-driven jet are plotted for early and late winter seasons in Figure 4, including distributions for all years and ENSO phase subsets; differences between the distributions during ENSO phases are also shown (Figure 4c,d). The distributions for all years in both early and late winter show the familiar trimodal jet latitude distribution highlighted in previous studies, with the jet preferentially located in southern, central, and northern locations (e.g., Woollings et al., 2010, 2014). Comparing the winter climatological distributions (i.e., grey lines in Figure 4a,b), it is clear that the jet tends to occur in the southern position more frequently in the late winter compared with the early winter, during which the jet tends to occur more frequently in the northern position.

Examining the distributions during the ENSO phases, the most substantial differences are seen in early winter, for which the modal jet position is in the central jet peak (around 45°N) during El Niño winters. In contrast, the jet is found in the northern position significantly more frequently during La Niña winters. In late winter, the eddy-driven jet is found in the southern position more frequently during El Niño winters at the expense of the more poleward positions, however, the ENSO differences are only marginally significant and smaller than the differences in the early winter. The clear difference in jet latitude distribution in early winter is particularly notable because it demonstrates that ENSO substantially influences the occurrence of the jet in its favoured positions, rather than an average shift in the distribution. The changes in occurrence frequency in response to ENSO are reminiscent of the behaviour of a simple nonlinear dynamical system in response to an external forcing (e.g., Palmer, 1999). Overall, this analysis highlights that changes in the distribution of the eddy-driven jet latitude on daily timescales are important to understand how the seasonal mean differences are established.

3.3 | Changes in the lifecycle of the early winter North Atlantic storm track and eddy-driven jet in response to ENSO

To understand why the influence of ENSO on the North Atlantic eddy-driven jet latitude distributions is so different between the early and late winter, we now examine the lifecycle of the North Atlantic storm track and associated changes in the downstream eddy-driven jet. Here we follow the approach of Novak et al. (2015), who

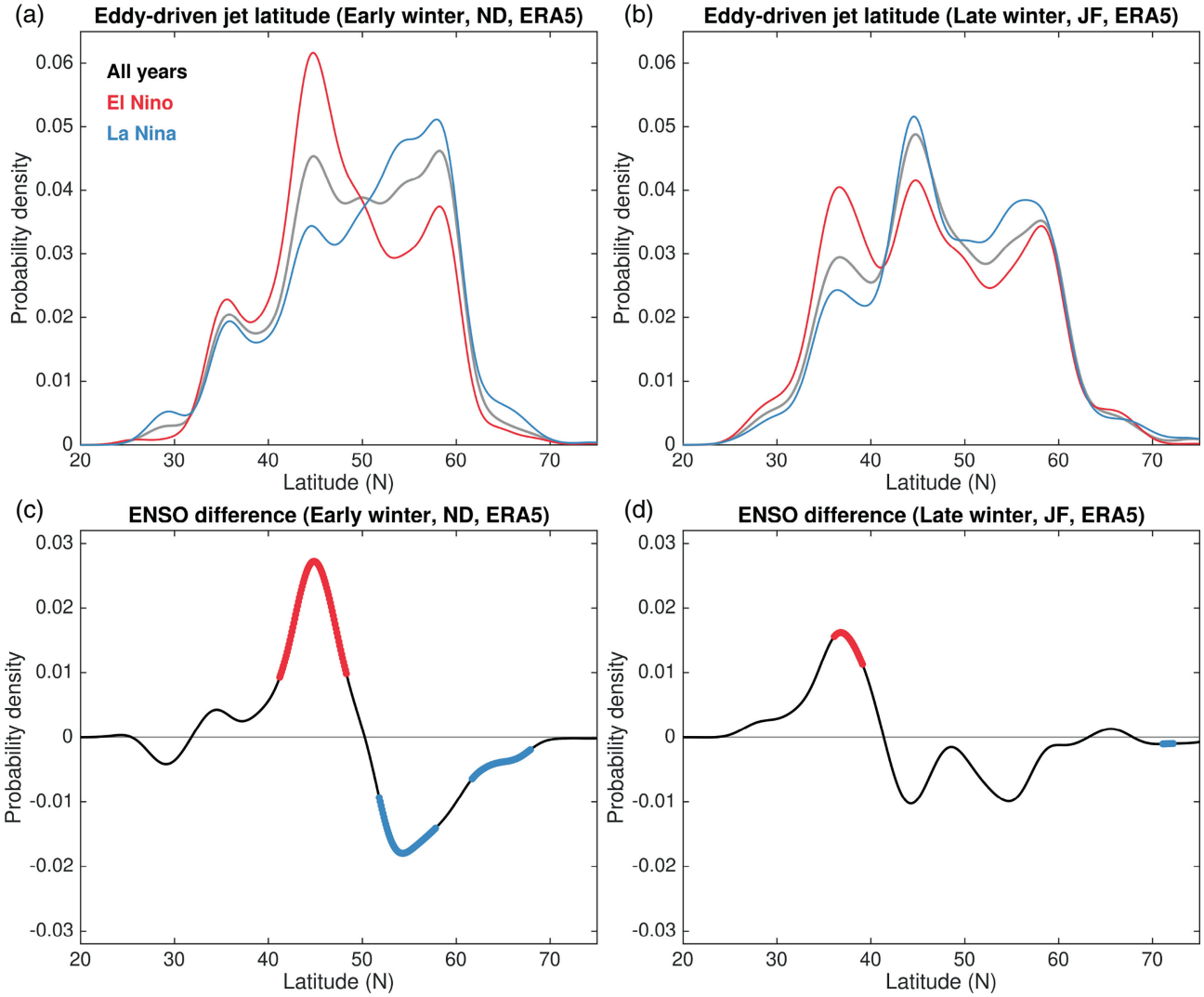

FIGURE 4 Eddy-driven jet latitude distributions for (a) early winter, ND, and (b) late winter, JF. In (a,b) the different curves show the distributions for all winters as well as El Niño and La Niña winters. (c,d) The difference between the eddy-driven jet latitude distributions for El Niño and La Niña winters. In (c,d) the curves are coloured where the difference has *p*-values less than 0.1: red indicates where the jet occurs more often during El Niño winters and blue indicates where the jet occurs more often during La Niña winters.

showed that poleward jet excursions in the North Atlantic tend to follow periods of intense storm-track activity over the western North Atlantic. We analyse composite high eddy heat flux events—identified as peaks in the 10-day low-pass filtered $\overline{v'T'}$ at 850 hPa—over the climatological storm track maximum region (35–50°N, 70–40°W; shown in Figure 2a,b). Events are defined as peaks in the eddy heat flux time series that exceed 25 $K{\cdot}m{\cdot}s^{-1}$ in early winter and 30 $K{\cdot}m{\cdot}s^{-1}$ in late winter and are separated by at least 10 days (the results that follow are not qualitatively sensitive to changes in these thresholds of $+/-5\,K{\cdot}m{\cdot}s^{-1}$ in either direction). These definitions result in a total of 118 events in early winter and 93 events in late winter.

Composites of the downstream eddy-driven jet (u at 850 hPa, between 0 and 30°W) are plotted in Figure 5a,b and the associated eddy heat flux event composites are shown in Figure 5c,d. In both early and late winter periods the eddy-driven jet is substantially further poleward on average following strong upstream eddy heat flux events, in agreement with the results shown by Novak et al. (2015). To examine how ENSO phase affects this behaviour, we subset the high heat flux events into El Niño and La Niña winters. In the early winter period, the jet is substantially further poleward following the high heat flux events during La Niña years, whereas the jet is further south during El Niño (i.e., Figure 5a). The jet displacement differences seen in early winter are consistent with the mean seasonal response to ENSO in early winter (i.e., Figures 1e and 4a,c), indicating that differences in the subseasonal evolution of the North Atlantic storm track and jet stream play an

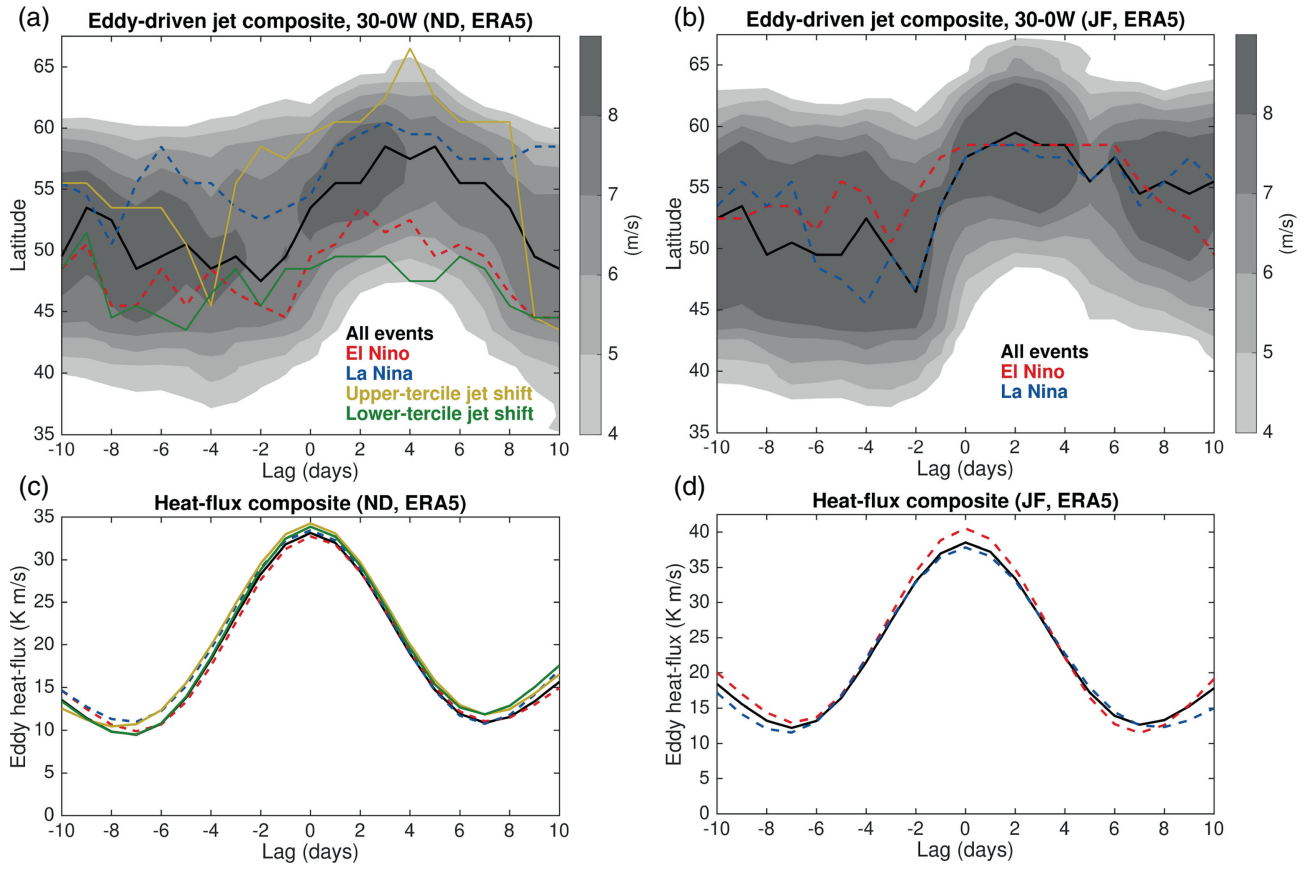

FIGURE 5 Downstream eddy-driven jet composites, defined as u at 850 hPa zonally averaged between 30W–0, averaged over high eddy heat flux events for (a) early winter, ND and (b) late winter, JF. The lines in (a,b) show the latitude of the composite jet maximum for all events and different subsets of these events; shading shows the composite average of all events. (c,d) The composite eddy heat flux ($\overline{v'T'}$ at 850 hPa, averaged over the region 35–50°N and 70–40°W) during the high eddy heat flux events. The eddy heat flux timeseries is 10-day low-pass filtered prior to selecting the peak events.

important role in establishing the seasonal mean ENSO teleconnection in early winter.

Interestingly, the composites of the upstream eddy heat flux are essentially indistinguishable between the ENSO phases (Figure 5c), indicating that differences in the downstream jet displacement are not due to the magnitude of the upstream eddy heat flux. In contrast to the early winter period, there is no clear difference in the composite jet evolution between ENSO phases in the late winter (Figure 5b).

We now focus our attention on the early winter period, when there is a stronger ENSO influence on the North Atlantic eddy-driven jet. To explore what determines the position of the downstream eddy-driven jet, we examine events where the downstream jet is displaced further north or south following high eddy heat flux events. To do this, we define subsets of events where the latitude of the downstream jet, averaged between 2 and 7 days after the heat flux peak, is in the upper and lower tercile of all events. For the early winter, there are 118 high eddy heat flux events in total, with subsets of 40 of these events making up the high/low jet shift composites. The composite evolution of the jet position during these subsets is shown in Figure 5a; the two subsets exhibit a clear difference in the downstream jet position, by construction. Lag composite maps of the lower-level zonal wind, EKE anomaly, and TEF anomaly are shown in Figure 6 for the upper-tercile jet shift events and lower-tercile jet shift events; maps of the differences between the upper- and lower-tercile composites are shown in Figure 7.

During the heat flux event peak (i.e., lag −1 to +1 days) and following the event (i.e., lag +2 to +4 days) the composites over the North Atlantic demonstrate a clear separation into a more northward/southward evolution of the eddy-driven jet (i.e., u_{850}), which is by construction. It is notable, however, that during the onset of the event (lag −1 to +1 days) the EKE is similar over most of the North Atlantic storm track in both composites, consistent with the similar eddy heat flux during the events (i.e., Figure 5c); substantial differences in EKE over the North

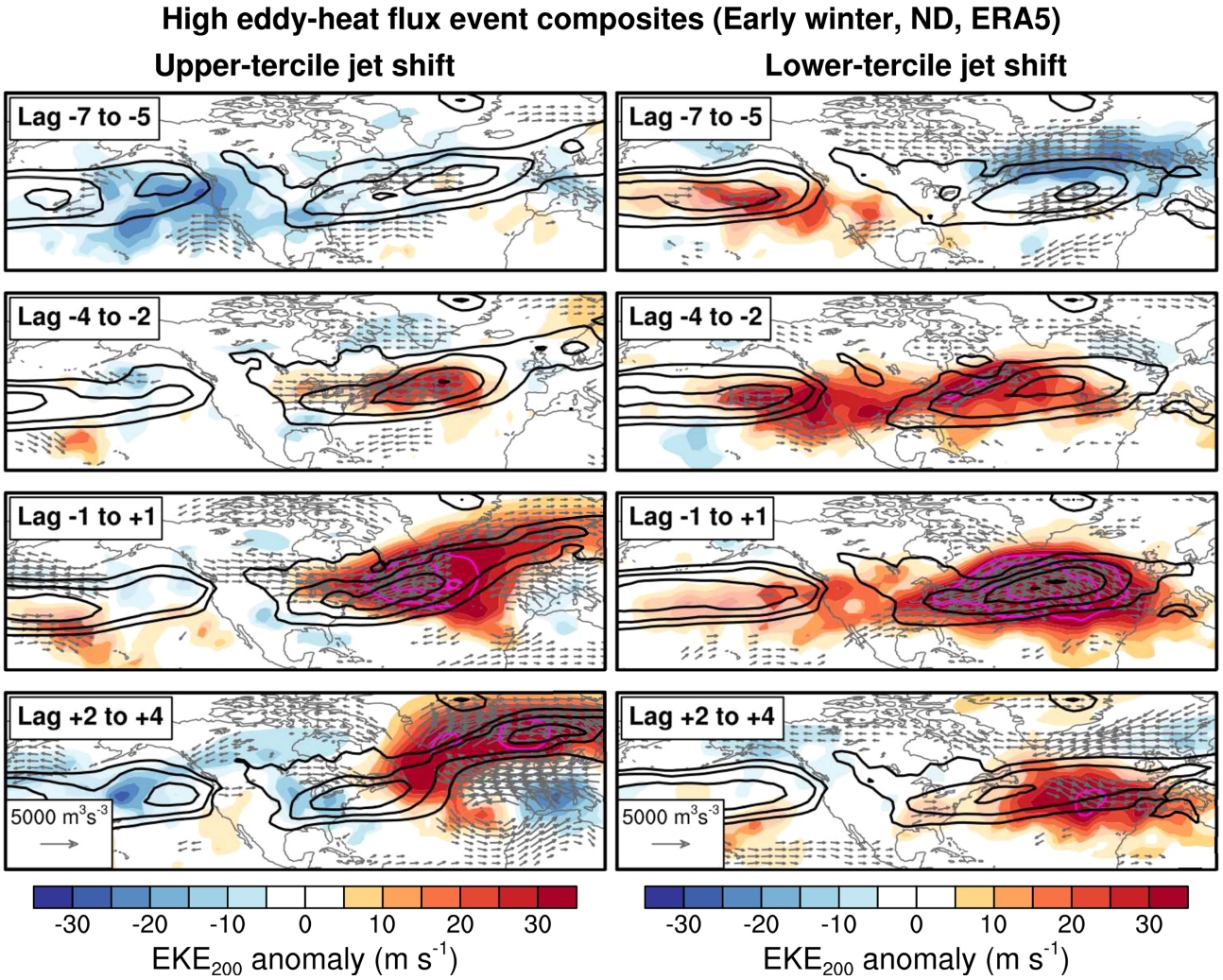

FIGURE 6 Evolution of the high eddy heat flux event composites for the upper-tercile jet shifts (left column) and lower-tercile jet shifts (right column). The EKE anomaly is shaded and the TEF anomaly is shown in vectors. The lower-level zonal wind (u at 850 hPa) is shown in contours, with intervals 2.5 m·s^{-1} from 5 m·s^{-1}. EKE anomaly contours for +40 and +60 m^2·s^{-2} are plotted in magenta beyond where the colour scale saturates. The lighter shaded regions indicate where the EKE anomaly has a p-value less than 0.1. The TEF vectors are only plotted where the zonal component has p-values less than 0.1.

Atlantic only emerge downstream at lag +2 to +4 days, which also reflect the jet shift itself.

Arguably the most interesting features of these composites are the upstream differences, over the eastern North Pacific and North America, prior to the onset of the high heat flux events. In the lower-tercile jet shift events, there are substantial positive EKE anomalies and positive zonal TEF anomalies present close to the west coast of North America at lag −7 to −5 days (Figure 6). These anomalies strengthen and seem to progress across North America at lag −4 to −2 days prior to the high heat flux events. The precursor anomalies seen in the lower-tercile jet shift events are absent in the upper-tercile jet shift events, with more negative EKE and TEF anomalies present over the eastern North Pacific. The difference between the two subset composites clearly highlights that there are precursor differences upstream, which are particularly strong over the eastern North Pacific (Figure 7). There are also some significant precursors over the North Atlantic itself at lag −7 to −5 days, suggesting that the existing circulation anomalies can also influence the magnitude of the downstream North Atlantic jet. Analysis of precursor North Pacific zonal wind anomalies (Figure S4) reveals a weaker signal that that seen for the EKE of the TEF anomalies, indicating that the upstream storm-track anomalies are particularly important in governing the downstream response over the North Atlantic. Examination of the **E**-vector composites during the high heat flux events (shown in Figure S5) reveals that there is strong anticyclonic wave breaking during the onset of the events (lag −1 to +1 days), which occurs further downstream in the lower-tercile jet subset (Figure 6). This is

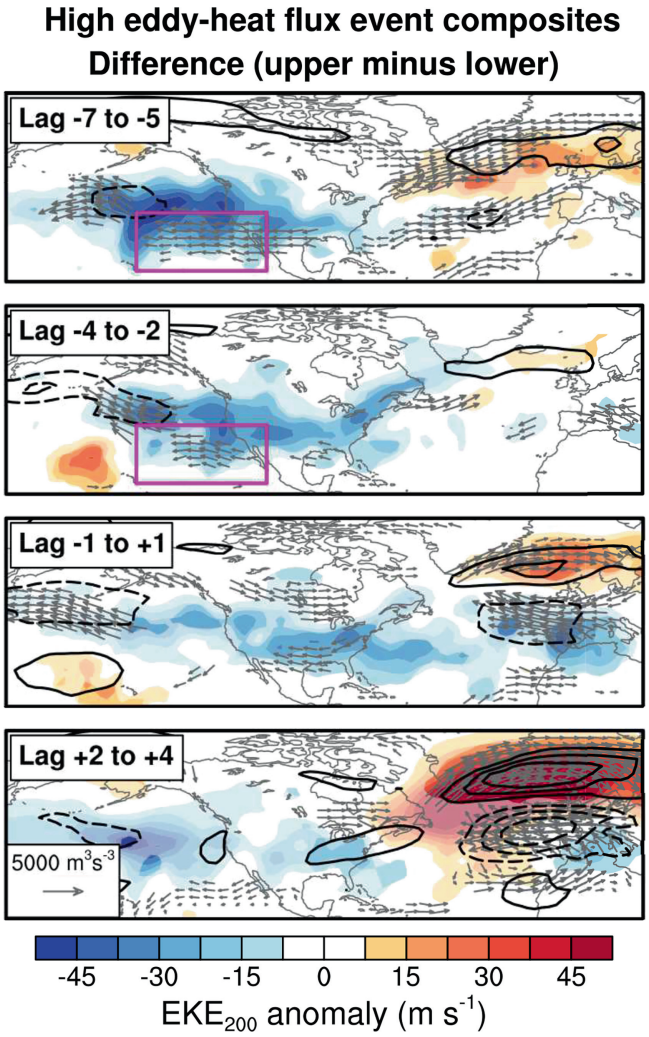

FIGURE 7 Difference between the evolution of the high eddy heat flux event composites for the upper-tercile jet shifts and lower-tercile jet shifts shown in Figure 6 (difference defined as upper-tercile minus lower-tercile). The EKE difference is shaded and the TEF difference is shown in vectors. The lower-level zonal wind difference (u at 850 hPa) is shown in contours, with intervals of 3 m·s^{-1} with negative values dashed and the zero contour suppressed. The lighter shaded regions indicate where the EKE difference has a p-value less than 0.1. The TEF vectors are only plotted where the zonal component has p-values less than 0.1.

associated with stronger momentum flux convergence by the eddies that act to reinforce the jet further south in these composites (Figure S6).

Overall, the composite analysis of high heat flux events highlights the apparent importance of the precursor anomalies propagating from upstream over the North Pacific and across North America during early winter. When there are stronger EKE/TEF anomalies upstream, the subsequent evolution of the growing synoptic waves in the North Atlantic tends to favour anticyclonic wave breaking further downstream and a more southward Atlantic jet position. In the absence of these strong precursor anomalies, growing synoptic waves tend to favour a shift of the jet into a more northward Atlantic jet position.

If we compare the precursor EKE and TEF anomalies during the high heat flux events with the mean ENSO teleconnection maps in Figure 2c,e, the anomalies clearly map onto the region of mean ENSO influence over the eastern North Pacific (highlighted by the magenta boxes). An equivalent precursor analysis in late winter shows weaker links to precursor anomalies, which do not clearly map onto the ENSO anomalies (Figure S7). The correspondence of the early winter precursor anomalies and the seasonal mean ENSO anomalies suggests a consistent mechanism through which the influence of ENSO in the North Pacific is linked to anomalies in the North Atlantic. In El Niño years, the North Pacific jet exhibits a stronger zonal extension of the jet and storm track (i.e., Figures 1e, 2c,e), driving the occurrence of the precursor conditions important for the more southward jet conditions in the North Atlantic (i.e., Figure 6). In La Niña years, the occurrence of these precursor conditions is less likely and the synoptic wave growth seems to be more independent and self-contained within the North Atlantic—under these conditions the high heat flux events in the North Atlantic storm track are more likely to lead to northward jet displacements.

To assess this influence on the seasonal timescale more directly, we now analyse the relationship between the eastern North Pacific storm track and the downstream North Atlantic jet averaged over the early winter period (shown in Figure 8). The North Pacific storm-track index is defined as the seasonal mean zonal TEF anomaly in the eastern North Pacific region (box shown in Figures 2e and 6). The North Atlantic jet index is defined as the difference in u at 850 hPa averaged between two boxes over the eastern North Atlantic (shown in Figure 1e), with positive values indicative of a more poleward jet and negative values indicative of a more equatorward jet (this is closely correlated with the East Atlantic pattern and analysis with this yields similar results, Figure S8). Here we focus on the TEF index in the North Pacific based on the composite analysis, but on the seasonal timescale this is strongly correlated with the upper-level zonal wind, such that an equivalent analysis reveals equivalent results (Figure S9).

Across the 72 early winter periods in the reanalysis, there is a clear and significant relationship with a negative correlation, $r = -0.57$, between the eastern North Pacific circulation anomalies and the downstream North Atlantic jet anomalies. When there is stronger TEF in the eastern North Pacific, the North Atlantic jet tends to be in a more southern position, consistent with the ENSO composite plots in Figures 1 and 2 and the heat flux event composites in Figure 6.

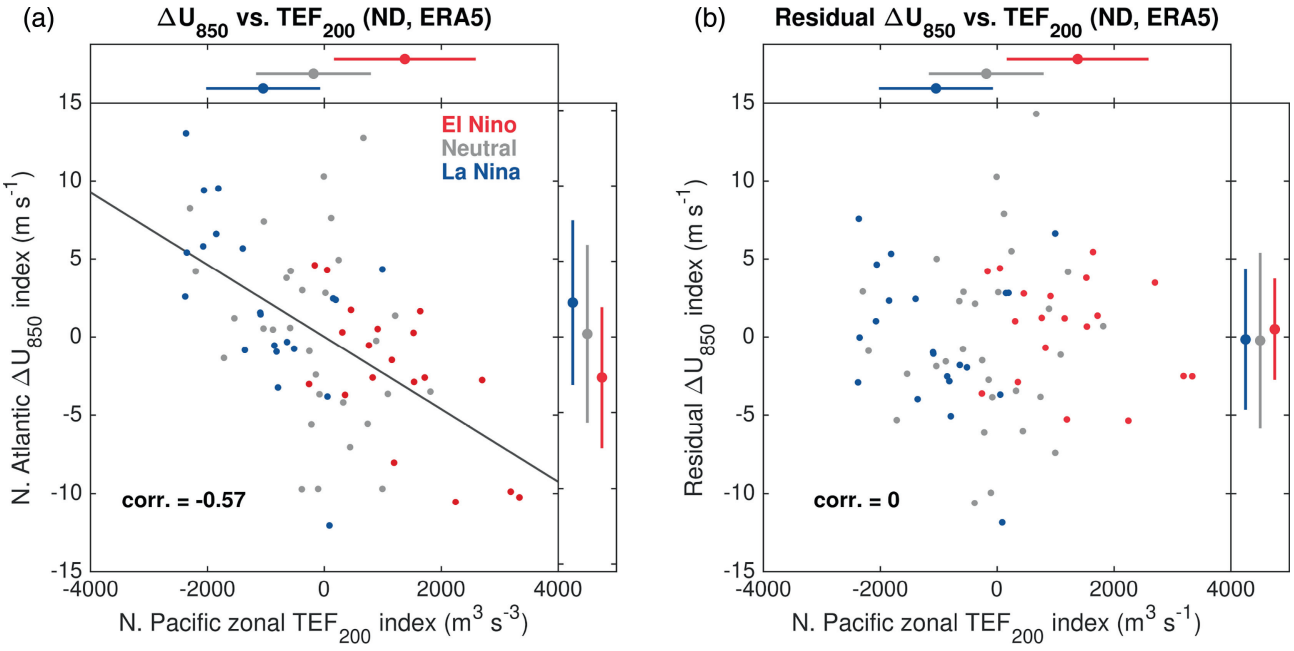

FIGURE 8 Scatter plot demonstrating the relationship between the North Atlantic jet index and the North Pacific TEF index. The North Atlantic jet index is defined as the difference in u at 850 hPa between the southern and northern boxes in Figure 1e. The North Pacific TEF index is defined as the average of the zonal component of the TEF over the downstream North Pacific region shown in Figures 2e and 6. The colours of the marks indicate the El Niño, La Niña, and Neutral winters. The adjacent plots indicate the average of each index over the different ENSO phases, with the lines indicating the +/- 1 standard deviation range. (b) As in (a) but for the residual North Atlantic jet index, where the linear influence of the North Pacific TEF index (indicated by the line of best fit in panel a) has been removed from the North Atlantic jet index.

Also shown in Figure 8 is a measure of each index average over El Niño, La Niña, and neutral years, along with the standard deviation. As expected, the clear influence of ENSO phase is evident in both indices. Using this linear relationship, we define a residual North Atlantic jet index by linearly regressing out the influence of the North Pacific index using a least-squares best-fit relationship (i.e., the line shown in Figure 8a). The plot of the residual North Atlantic jet index against the North Pacific zonal TEF index is shown in Figure 8b. The averages of the residual North Atlantic jet index over El Niño, La Niña, and neutral years are essentially indistinguishable, indicating that the systematic influence of ENSO on the North Atlantic jet in the early winter season can be largely explained statistically—or "mediated"—through the influence of ENSO on the storm track and jet in the eastern North Pacific.

3.4 | Links to changes in blocking frequency during different phases of ENSO

The early winter ENSO teleconnection is characterised by changes in the frequency of poleward jet excursions and these are reminiscent of the persistent wintertime ridging/blocking events highlighted in previous studies. In this subsection we will briefly assess the role of blocking over the North Atlantic sector in contributing to the ENSO teleconnection patterns.

We examine the changes in blocking frequency between the two ENSO phases by calculating a common two-dimensional $Z500$ blocking index (see Section 2); the ENSO differences in early and late winter are shown in Figure 9. In the early winter there is significantly more blocking near the Iberian peninsula in the La Niña years (Figure 9a), when the North Atlantic eddy-driven jet is located in the northern position more frequently (i.e., Figure 4a). This is consistent with the dynamical relationship highlighted by Woollings et al. (2011), who found that during the DJF winter months the northward jet displacements over the North Atlantic are associated with large-scale Rossby wave breaking around the Iberian Peninsula (or "Iberian wave-breaking events"). In their study, the blocking events were found to increase the persistence of the northward jet displacements compared with more common ridging events. In the late winter, there is significantly more blocking over Greenland in El Niño years (Figure 9b), which is associated with the North Atlantic eddy-driven jet being located in the southern position more frequently (i.e., Figure 4b) and

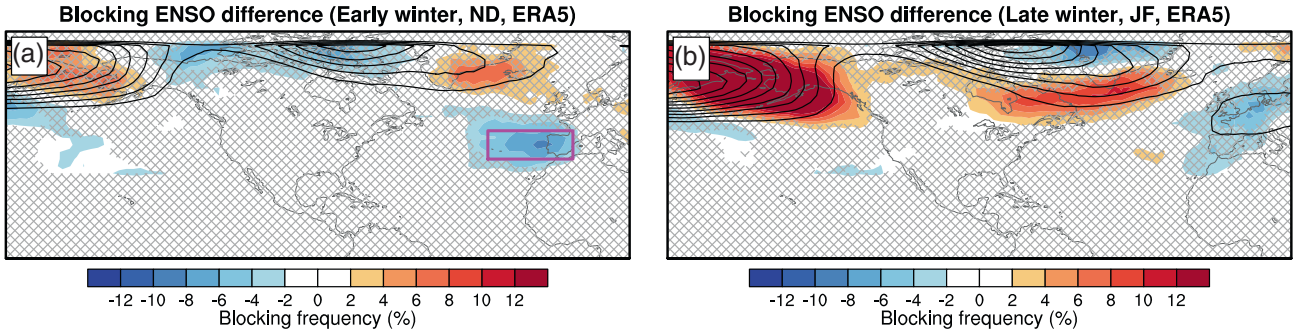

FIGURE 9 Difference between El Niño and La Niña phases in early winter, ND, and late winter, JF, for the blocking frequency (calculated using a two-dimensional $Z500$ wave-breaking index; see Section 2). The climatologies (1950–2022) for the different periods are contoured, with contour intervals of 5%, starting from 10%. Hatching indicates regions where the difference (shaded) has a p-value greater than 0.1.

negative NAO-like anomalies (i.e., Figure 1b), consistent with previous studies on the association of Greenland blocking, eddy-driven jet, and NAO (e.g., Woollings et al., 2010).

Analysing the composite evolution of early winter Iberian wave-breaking events reveals an increase in the eddy heat flux upstream preceding the onset of these events (Figure S10), consistent with the northward jet displacements seen following high eddy heat flux events (i.e., Figure 3c). Prior to these events there are EKE anomalies over North America similar to those seen in the high heat flux event composites (i.e., Figures 6 and 7) and the seasonal mean ENSO anomalies (i.e., Figure 2c). Analysis of these composites provides further evidence that precursor anomalies upstream over the eastern North Pacific and North America are important in determining the likelihood of poleward jet displacements over the North Atlantic and why these are more likely when the storm-track anomalies are relatively weak across the southern part of North America, as seen in La Niña years.

4 | SUMMARY AND DISCUSSION

In this study we have revisited the intraseasonal variability of the ENSO teleconnection in the North Atlantic. As found in previous studies, there are distinct differences in the mean large-scale circulation response to ENSO between early winter (ND) and late winter (JF). Here we have identified distinct differences in the storm-track dynamics that characterise the North Atlantic response to ENSO in early and late winter.

The clearest and statistically strongest response to ENSO is found in early winter and is associated with significantly less frequent northern jet occurrences in El Niño years and significantly more frequent northern jet occurrences in La Niña years (i.e., Figure 4). These poleward jet excursions typically follow peaks in the upstream eddy heat flux (Figure 5a), however, in El Niño years this relationship breaks down and the jet does not transition to the northern position as frequently, despite no clear changes in the upstream eddy heat flux (Figure 5c).

Further analysis reveals that high heat flux events that are not followed by a poleward jet displacement tend to be preceded by a stronger than average EKE and downstream TEF in the eastern North Pacific and over North America (Figure 6). In contrast, the events with the strongest poleward jet displacements are preceded by weakly negative EKE and downstream TEF anomalies. These precursors map onto the seasonal mean ENSO influence on the North Pacific jet and storm track. Analysis of the mean early winter relationship between the TEF in the eastern North Pacific and the eddy-driven jet in the eastern North Atlantic reveals that the ENSO jet anomalies in the North Atlantic can be entirely explained through the storm-track activity in the eastern North Pacific (Figure 7).

The late winter response is associated with a zonally consistent southward shift of the North Pacific and North Atlantic upper-level jet and storm track during El Niño winters and favours negative NAO conditions, though it is weaker statistically than the early winter response. The late winter circulation response in the North Atlantic is linked to a strengthening of the downstream TEF across Mexico (Figure 2f) and is reinforced by a clear increase in cyclonic wave breaking in the North Atlantic (Figure 3); both of these are consistent with previous studies focusing on the late winter teleconnection (e.g., Drouard et al., 2015; Jiménez-Esteve & Domeisen, 2020; Seager, Naik, et al., 2010).

As well as these tropospheric mechanisms, previous studies have also highlighted the influence of the stratospheric polar vortex in governing the late North Atlantic response to ENSO (e.g., Ayarzagüena et al., 2018; Domeisen et al., 2019; Hardiman et al., 2019). Whilst it

is clear that winters with sudden stratospheric warming (SSW) events tend to be strongly associated with negative NAO conditions, the relationship between ENSO and the occurrence of SSW events is quite weak and uncertain (Domeisen et al., 2019; Garfinkel et al., 2012; Lockwood et al., 2022; Polvani et al., 2017). The role of the stratosphere and the uncertainty of its response provide a possible explanation of why the late winter teleconnection to the North Atlantic is statistically weaker than in early winter. SSWs occur much less frequently in the early winter (e.g., Butler et al., 2017) and there is a delayed response of the tropospheric circulation to SSW events. Therefore, the impact of SSW events on the North Atlantic circulation—and likewise on the uncertainty of the circulation—is substantially lower during the early winter than in the late winter. In the absence of this stratospheric influence it is possible that the tropospheric pathway through which ENSO influences the North Atlantic circulation is relatively unencumbered compared with the late winter.

Our analysis indicates that the different response of the North Atlantic circulation to ENSO in early and late winter is associated with very different anomalies in the direction of synoptic wave breaking over the North Atlantic (i.e., Figure 3). Our results show that in the late winter the increased cyclonic wave breaking found over the North Atlantic (Figure 3f) is associated with an upstream zonal jet that is substantially further south and more zonal as it enters the North Atlantic basin compared with the early winter (Figure 1d). Idealised studies have previously shown that shifting a baroclinic jet further south tends to increase the occurrence of cyclonic wave breaking, whereas anticyclonic wave breaking tends to dominate when jets are located further north (Drouard et al., 2013; Rivière, 2009). The clear differences in the upstream climatological jet in late winter could therefore be responsible for producing the differences in the ENSO responses seen here in late winter, associated with the southward seasonal march of the jet stream location between early and late winter (e.g. Figure 1c,d)—this tends to increase the cyclonic wind shear of the climatological jet in late winter, as shown by Geng et al. (2023), which in turn favours cyclonic wave breaking (e.g., Rivière, 2009).

Some further consideration of the seasonal dependence of the North Atlantic jet and SLP variability may provide insight into the origins of the early/late winter differences. In the early winter period the jet is located in the southern position much less frequently and the majority of the jet variability is between the central and northern positions (Figure S11), whereas in late winter the southern position occurs more frequently and is more important in governing the overall jet variability. There are associated changes in the leading patterns of variability in SLP over the North Atlantic, specifically the first and second empirical orthogonal function (EOF) patterns corresponding to the North Atlantic Oscillation (NAO) and the East Atlantic pattern (EA), respectively (Figure S12). Similar patterns of SLP anomaly are apparent in both early and late winter; however, there are distinct differences in the fraction of variance explained by each mode. In early winter, the NAO and EA account for fairly comparable amounts of the total variance explained ($NAO_{ND} = 31.9\%$, $EA_{ND} = 26.0\%$). Contrastingly, in late winter, the NAO accounts for more than double the amount of total variance explained compared with the EA ($NAO_{JF} = 41.2\%$, $EA_{JF} = 18.8\%$). The NAO dominates the variability in late winter and most of the ENSO teleconnection to the North Atlantic projects onto the NAO pattern, as shown by King et al. (2023); however, the NAO is much less dominant in early winter, which could explain why the ENSO teleconnection pattern is able to project so clearly on the East Atlantic pattern in early winter, when the North Atlantic jet variability is mostly constrained within the more northern parts of the basin.

In the early winter, the behaviour of the eddy-driven jet is characterised by the intermittent influence of anomalies upstream over the North Pacific (i.e., Figure 6), which may be due to the clearer separation between the Pacific and Atlantic jet (i.e., Figure 1c). In the absence of strong downstream propagation of eddy energy from the North Pacific, strong North Atlantic heat flux events tend to result in large poleward jet displacements, associated with Iberian wave-breaking events, whereas in the presence of stronger downstream propagation of eddy energy the North Pacific jet exhibits a stronger connection to the North Atlantic (as in El Niño years) and high eddy heat flux events tend to force the eddy-driven jet in the central position (i.e., Figure 6). Developing a more detailed mechanistic understanding of the upstream Pacific influence on the North Atlantic jet in this early winter period is an important avenue for further research that is motivated by this study.

This study has demonstrated the important role of the North Pacific jet and storm track on the North Atlantic large-scale circulation on subseasonal-to-seasonal (S2S) timescales. The intraseasonal variability of the ENSO teleconnection to the North Atlantic demonstrated here should be an important source of skill in S2S forecasts—particularly during the early winter (ND) period, which has received less attention in the literature. The early winter ENSO teleconnection to the North Atlantic in operational seasonal forecast models (from the C3S ensemble) was examined in the recent studies by Molteni and Brookshaw (2023) and Thornton et al. (2023), with the latter demonstrating that there is significant skill originating from ENSO in operational seasonal forecasts of the early winter period. However, these studies also show

that models significantly underestimate the magnitude of the circulation response to ENSO compared with observations and thereby miss an important source of potentially predictable signal, though these studies did not address in detail the mechanisms underlying the ENSO teleconnection to the North Atlantic in these models. Revisiting the early winter teleconnection in operational seasonal forecast models to understand how they represent the important storm-track dynamics demonstrated in this study and, crucially, which aspects of the teleconnection are deficient in the models is a current focus of our ongoing research.

AUTHOR CONTRIBUTIONS

Christopher H. O'Reilly: conceptualization; formal analysis; funding acquisition; investigation; methodology; project administration; visualization; writing – original draft; writing – review and editing. **Marie Drouard:** conceptualization; investigation; methodology; writing – original draft; writing – review and editing. **Blanca Ayarzagüena:** conceptualization; investigation; methodology; writing – original draft; writing – review and editing. **Maarten H. P. Ambaum:** conceptualization; investigation; methodology; writing – original draft; writing – review and editing. **John Methven:** conceptualization; investigation; methodology; writing – original draft; writing – review and editing.

ACKNOWLEDGEMENTS

C. O'Reilly was supported by a Royal Society University Research Fellowship (URF\R1\201230).

DATA AVAILABILITY STATEMENT

The data that support the findings of this study are available publicly from ECMWF (ERA5, atmospheric reanalysis) and the Met Office (HadISST, global gridded observed SST product).

ORCID

Christopher H. O'Reilly https://orcid.org/0000-0002-8630-1650
Blanca Ayarzagüena https://orcid.org/0000-0003-3959-5673
Maarten H. P. Ambaum https://orcid.org/0000-0002-6824-8083

REFERENCES

Abid, M.A., Kucharski, F., Molteni, F. & Almazroui, M. (2023) Predictability of Indian Ocean precipitation and its North Atlantic teleconnections during early winter. *Npj Climate and Atmospheric Science*, 6(1), 1–10. Available from: https://doi.org/10.1038/s41612-023-00328-z

Abid, M.A., Kucharski, F., Molteni, F., Kang, I.-S., Tompkins, A.M. & Almazroui, M. (2021) Separating the Indian and Pacific Ocean impacts on the euro-Atlantic response to ENSO and its transition from early to late winter. *Journal of Climate*, 34(4), 1531–1548. Available from: https://doi.org/10.1175/JCLI-D-20-0075.1

Ambaum, M.H.P. (2010) Significance tests in climate science. *Journal of Climate*, 23(22), 5927–5932. Available from: https://doi.org/10.1175/2010JCLI3746.1

Ambaum, M.H.P. & Novak, L. (2014) A nonlinear oscillator describing storm track variability. *Quarterly Journal of the Royal Meteorological Society*, 140(685), 2680–2684. Available from: https://doi.org/10.1002/qj.2352

Ayarzagüena, B., Ineson, S., Dunstone, N.J., Baldwin, M.P. & Scaife, A.A. (2018) Intraseasonal effects of El Niño–southern oscillation on North Atlantic climate. *Journal of Climate*, 31(21), 8861–8873. Available from: https://doi.org/10.1175/JCLI-D-18-0097.1

Brönnimann, S., Xoplaki, E., Casty, C., Pauling, A. & Luterbacher, J. (2007) ENSO influence on Europe during the last centuries. *Climate Dynamics*, 28(2), 181–197. Available from: https://doi.org/10.1007/s00382-006-0175-z

Butler, A.H., Polvani, L.M. & Deser, C. (2014) Separating the stratospheric and tropospheric pathways of El Niño–southern oscillation teleconnections. *Environmental Research Letters*, 9(2), 024014. Available from: https://doi.org/10.1088/1748-9326/9/2/024014

Butler, A.H., Sjoberg, J.P., Seidel, D.J. & Rosenlof, K.H. (2017) A sudden stratospheric warming compendium. *Earth System Science Data*, 9(1), 63–76. Available from: https://doi.org/10.5194/essd-9-63-2017

Cook, E.R., Seager, R., Cane, M.A. & Stahle, D.W. (2007) North American drought: reconstructions, causes, and consequences. *Earth-Science Reviews*, 81(1), 93–134. Available from: https://doi.org/10.1016/j.earscirev.2006.12.002

Domeisen, D.I., Garfinkel, C.I. & Butler, A.H. (2019) The teleconnection of El Niño southern oscillation to the stratosphere. *Reviews of Geophysics*, 57(1), 5–47. Available from: https://doi.org/10.1029/2018RG000596

Drouard, M., Rivière, G. & Arbogast, P. (2013) The North Atlantic oscillation response to large-scale atmospheric anomalies in the northeastern pacific. *Journal of the Atmospheric Sciences*, 70(9), 2854–2874. Available from: https://doi.org/10.1175/JAS-D-12-0351.1

Drouard, M., Rivière, G. & Arbogast, P. (2015) The link between the north pacific climate variability and the North Atlantic oscillation via downstream propagation of synoptic waves. *Journal of Climate*, 28(10), 3957–3976. Available from: https://doi.org/10.1175/JCLI-D-14-00552.1

Duchon, C.E. (1979) Lanczos filtering in one and two dimensions. *Journal of Applied Meteorology and Climatology*, 18(8), 1016–1022. Available from: https://doi.org/10.1175/1520-0450(1979)018<1016:LFIOAT>2.0.CO;2

Dunstone, N., Smith, D., Scaife, A., Hermanson, L., Eade, R., Robinson, N. et al. (2016) Skilful predictions of the winter North Atlantic oscillation one year ahead. *Nature Geoscience*, 9(11), 809–814. Available from: https://doi.org/10.1038/ngeo2824

Garfinkel, C.I., Butler, A.H., Waugh, D.W., Hurwitz, M.M. & Polvani, L.M. (2012) Why might stratospheric sudden warmings occur with similar frequency in El Niño and La Niña winters? *Journal of Geophysical Research: Atmospheres*, 117, D19106. Available from: https://doi.org/10.1029/2012JD017777

Geng, X., Zhao, J. & Kug, J.-S. (2023) ENSO-driven abrupt phase shift in North Atlantic oscillation in early January. *Npj Climate and*

Atmospheric Science, 6(1), 1–8. Available from: https://doi.org/10.1038/s41612-023-00414-2

Hardiman, S.C., Dunstone, N.J., Scaife, A.A., Smith, D.M., Ineson, S., Lim, J. et al. (2019) The impact of strong El Niño and La Niña events on the North Atlantic. *Geophysical Research Letters*, 46(5), 2874–2883. Available from: https://doi.org/10.1029/2018GL081776

Hersbach, H., Bell, B., Berrisford, P., Hirahara, S., Horányi, A., Muñoz-Sabater, J. et al. (2020) The ERA5 global reanalysis. *Quarterly Journal of the Royal Meteorological Society*, 146(730), 1999–2049. Available from: https://doi.org/10.1002/qj.3803

Horel, J.D. & Wallace, J.M. (1981) Planetary-scale atmospheric phenomena associated with the southern oscillation. *Monthly Weather Review*, 109(4), 813–829. Available from: https://doi.org/10.1175/1520-0493(1981)109<0813:PSAPAW>2.0.CO;2

Hoskins, B.J., James, I.N. & White, G.H. (1983) The shape, propagation and mean-flow interaction of large-scale weather systems. *Journal of the Atmospheric Sciences*, 40(7), 1595–1612. Available from: https://doi.org/10.1175/1520-0469(1983)040<1595:TSPAMF>2.0.CO;2

Hurrell, J.W., Kushnir, Y., Ottersen, G. & Visbeck, M. (2003) An overview of the North Atlantic oscillation. In: *The North Atlantic oscillation: climatic significance and environmental impact*. American Geophysical Union (AGU), pp. 1–35. Available from: https://doi.org/10.1029/134GM01

Ineson, S. & Scaife, A.A. (2009) The role of the stratosphere in the European climate response to El Niño. *Nature Geoscience*, 2(1), 32–36. Available from: https://doi.org/10.1038/ngeo381

Jiménez-Esteve, B. & Domeisen, D.I.V. (2018) The tropospheric pathway of the ENSO–North Atlantic teleconnection. *Journal of Climate*, 31(11), 4563–4584. Available from: https://doi.org/10.1175/JCLI-D-17-0716.1

Jiménez-Esteve, B. & Domeisen, D.I.V. (2020) Nonlinearity in the tropospheric pathway of ENSO to the North Atlantic. *Weather and Climate Dynamics*, 1(1), 225–245. Available from: https://doi.org/10.5194/wcd-1-225-2020

King, M.P., Herceg-Bulić, I., Bladé, I., García-Serrano, J., Keenlyside, N., Kucharski, F. et al. (2018) Importance of late fall ENSO teleconnection in the euro-Atlantic sector. *Bulletin of the American Meteorological Society*, 99(7), 1337–1343. Available from: https://doi.org/10.1175/BAMS-D-17-0020.1

King, M.P., Keenlyside, N. & Li, C. (2023) ENSO teleconnections in terms of non-NAO and NAO atmospheric variability. *Climate Dynamics*, 61(5), 2717–2733. Available from: https://doi.org/10.1007/s00382-023-06697-8

Li, Y. & Lau, N.-C. (2012) Impact of ENSO on the atmospheric variability over the North Atlantic in late winter—role of transient eddies. *Journal of Climate*, 25(1), 320–342. Available from: https://doi.org/10.1175/JCLI-D-11-00037.1

Lockwood, J.F., Stringer, N., Thornton, H.E., Scaife, A.A., Bett, P.E., Collier, T. et al. (2022) Predictability of European winter 2020/2021: influence of a mid-winter sudden stratospheric warming. *Atmospheric Science Letters*, 23(12), e1126. Available from: https://doi.org/10.1002/asl.1126

Masato, G., Hoskins, B.J. & Woollings, T. (2013) Wave-breaking characteristics of northern hemisphere winter blocking: a two-dimensional approach. *Journal of Climate*, 26(13), 4535–4549. Available from: https://doi.org/10.1175/JCLI-D-12-00240.1

Molteni, F. (2020) Boreal-winter teleconnections with tropical indo-Pacific rainfall in HighResMIP historical simulations from the PRIMAVERA project. *Climate Dynamics*, 55(7), 1843–1873. Available from: https://doi.org/10.1007/s00382-020-05358-4

Molteni, F. & Brookshaw, A. (2023) Early- and late-winter ENSO teleconnections to the euro-Atlantic region in state-of-the-art seasonal forecasting systems. *Climate Dynamics*, 61(5), 2673–2692. Available from: https://doi.org/10.1007/s00382-023-06698-7

Moron, V. & Gouirand, I. (2003) Seasonal modulation of the El Niño–southern oscillation relationship with sea level pressure anomalies over the North Atlantic in October–march 1873–1996. *International Journal of Climatology*, 23(2), 143–155. Available from: https://doi.org/10.1002/joc.868

Novak, L., Ambaum, M.H.P. & Tailleux, R. (2015) The life cycle of the North Atlantic storm track. *Journal of the Atmospheric Sciences*, 72(2), 821–833.

O'Reilly, C.H., Heatley, J., MacLeod, D., Weisheimer, A., Palmer, T.N., Schaller, N. et al. (2017) Variability in seasonal forecast skill of northern hemisphere winters over the twentieth century. *Geophysical Research Letters*, 44(11), 5729–5738. Available from: https://doi.org/10.1002/2017GL073736

O'Reilly, C.H., Minobe, S., Kuwano-Yoshida, A. & Woollings, T. (2017) The Gulf stream influence on wintertime North Atlantic jet variability. *Quarterly Journal of the Royal Meteorological Society*, 143(702), 173–183. Available from: https://doi.org/10.1002/qj.2907

O'Reilly, C.H., Weisheimer, A., MacLeod, D., Befort, D.J. & Palmer, T. (2020) Assessing the robustness of multidecadal variability in northern hemisphere wintertime seasonal forecast skill. *Quarterly Journal of the Royal Meteorological Society*, 146(733), 4055–4066. Available from: https://doi.org/10.1002/qj.3890

Orlanski, I. & Chang, E.K.M. (1993) Ageostrophic geopotential fluxes in downstream and upstream development of baroclinic waves. *Journal of the Atmospheric Sciences*, 50(2), 212–225. Available from: https://doi.org/10.1175/1520-0469(1993)050<0212:AGFIDA>2.0.CO;2

Palmer, T.N. (1999) A nonlinear dynamical perspective on climate prediction. *Journal of Climate*, 12(2), 575–591. Available from: https://doi.org/10.1175/1520-0442(1999)012<0575:ANDPOC>2.0.CO;2

Polvani, L.M., Sun, L., Butler, A.H., Richter, J.H. & Deser, C. (2017) Distinguishing stratospheric sudden warmings from ENSO as key drivers of wintertime climate variability over the North Atlantic and Eurasia. *Journal of Climate*, 30(6), 1959–1969. Available from: https://doi.org/10.1175/JCLI-D-16-0277.1

Pozo-Vázquez, D., Gámiz-Fortis, S.R., Tovar-Pescador, J., Esteban-Parra, M.J. & Castro-DÍez, Y. (2005a) North Atlantic winter SLP anomalies based on the autumn ENSO state. *Journal of Climate*, 18(1), 97–103. Available from: https://doi.org/10.1175/JCLI-3210.1

Pozo-Vázquez, D., Gámiz-Fortis, S.R., Tovar-Pescador, J., Esteban-Parra, M.J. & Castro-Díez, Y. (2005b) El Niño–southern oscillation events and associated European winter precipitation anomalies. *International Journal of Climatology*, 25(1), 17–31. Available from: https://doi.org/10.1002/joc.1097

Rayner, N.A., Parker, D.E., Horton, E.B., Folland, C.K., Alexander, L.V., Rowell, D.P. et al. (2003) Global analyses of sea surface

temperature, sea ice, and night marine air temperature since the late nineteenth century. *Journal of Geophysical Research: Atmospheres*, 108, 4407. Available from: https://doi.org/10.1029/2002JD002670

Rivière, G. (2009) Effect of latitudinal variations in low-level baroclinicity on eddy life cycles and upper-tropospheric wave-breaking processes. *Journal of the Atmospheric Sciences*, 66(6), 1569–1592. Available from: https://doi.org/10.1175/2008JAS2919.1

Scaife, A.A., Arribas, A., Blockley, E., Brookshaw, A., Clark, R.T., Dunstone, N. et al. (2014) Skillful long-range prediction of European and north American winters. *Geophysical Research Letters*, 41(7), 2514–2519. Available from: https://doi.org/10.1002/2014GL059637

Seager, R., Kushnir, Y., Nakamura, J., Ting, M. & Naik, N. (2010) Northern hemisphere winter snow anomalies: ENSO, NAO and the winter of 2009/10. *Geophysical Research Letters*, 37, L14703. Available from: https://doi.org/10.1029/2010GL043830

Seager, R., Naik, N., Ting, M., Cane, M.A., Harnik, N. & Kushnir, Y. (2010) Adjustment of the atmospheric circulation to tropical Pacific SST anomalies: variability of transient eddy propagation in the Pacific–North America sector. *Quarterly Journal of the Royal Meteorological Society*, 136(647), 277–296. Available from: https://doi.org/10.1002/qj.588

Silverman, B.W. (1981) Using kernel density estimates to investigate multimodality. *Journal of the Royal Statistical Society. Series B, Methodological*, 43(1), 97–99. Available from: https://doi.org/10.1111/j.2517-6161.1981.tb01155.x

Smith, D.M., Scaife, A.A. & Kirtman, B.P. (2012) What is the current state of scientific knowledge with regard to seasonal and decadal forecasting? *Environmental Research Letters*, 7(1), 015602. Available from: https://doi.org/10.1088/1748-9326/7/1/015602

Taschetto, A.S., Ummenhofer, C.C., Stuecker, M.F., Dommenget, D., Ashok, K., Rodrigues, R.R. et al. (2020) ENSO atmospheric teleconnections. In: *El Niño southern oscillation in a changing climate*. American Geophysical Union (AGU), pp. 309–335. Available from: https://doi.org/10.1002/9781119548164.ch14

Thornton, H.E., Smith, D.M., Scaife, A.A. & Dunstone, N.J. (2023) Seasonal predictability of the East Atlantic pattern in late autumn and early winter. *Geophysical Research Letters*, 50(1), e2022GL100712. Available from: https://doi.org/10.1029/2022GL100712

Toniazzo, T. & Scaife, A.A. (2006) The influence of ENSO on winter North Atlantic climate. *Geophysical Research Letters*, 33, L24704. Available from: https://doi.org/10.1029/2006GL027881

Trenberth, K.E. (1986) An assessment of the impact of transient eddies on the zonal flow during a blocking episode using localized eliassen-palm flux diagnostics. *Journal of the Atmospheric Sciences*, 43(19), 2070–2087. Available from: https://doi.org/10.1175/1520-0469(1986)043<2070:AAOTIO>2.0.CO;2

Trenberth, K.E. (2020) ENSO in the global climate system. In: *El Niño southern oscillation in a changing climate*. American Geophysical Union (AGU), pp. 21–37. Available from: https://doi.org/10.1002/9781119548164.ch2

Trenberth, K.E., Branstator, G.W., Karoly, D., Kumar, A., Lau, N.-C. & Ropelewski, C. (1998) Progress during TOGA in understanding and modeling global teleconnections associated with tropical sea surface temperatures. *Journal of Geophysical Research: Oceans*, 103(C7), 14291–14324. Available from: https://doi.org/10.1029/97JC01444

Vautard, R. (1990) Multiple weather regimes over the North Atlantic: analysis of precursors and successors. *Monthly Weather Review*, 118(10), 2056–2081. Available from: https://doi.org/10.1175/1520-0493(1990)118<2056:MWROTN>2.0.CO;2

Wallace, J.M. & Gutzler, D.S. (1981) Teleconnections in the geopotential height field during the northern hemisphere winter. *Monthly Weather Review*, 109(4), 784–812. Available from: https://doi.org/10.1175/1520-0493(1981)109<0784:TITGHF>2.0.CO;2

Woollings, T., Czuchnicki, C. & Franzke, C. (2014) Twentieth century North Atlantic jet variability. *Quarterly Journal of the Royal Meteorological Society*, 140(680), 783–791. Available from: https://doi.org/10.1002/qj.2197

Woollings, T., Hannachi, A. & Hoskins, B. (2010) Variability of the North Atlantic eddy-driven jet stream. *Quarterly Journal of the Royal Meteorological Society*, 136(649), 856–868. Available from: https://doi.org/10.1002/qj.625

Woollings, T., Hoskins, B., Blackburn, M. & Berrisford, P. (2008) A new Rossby wave–breaking interpretation of the North Atlantic oscillation. *Journal of the Atmospheric Sciences*, 65(2), 609–626. Available from: https://doi.org/10.1175/2007JAS2347.1

Woollings, T., Pinto, J.G. & Santos, J.A. (2011) Dynamical evolution of North Atlantic ridges and poleward jet stream displacements. *Journal of the Atmospheric Sciences*, 68(5), 954–963. Available from: https://doi.org/10.1175/2011JAS3661.1

SUPPORTING INFORMATION

Additional supporting information can be found online in the Supporting Information section at the end of this article.

How to cite this article: O'Reilly, C.H., Drouard, M., Ayarzagüena, B., Ambaum, M.H.P. & Methven, J. (2024) The role of storm-track dynamics in the intraseasonal variability of the winter ENSO teleconnection to the North Atlantic. *Quarterly Journal of the Royal Meteorological Society*, 150(761), 2069–2086. Available from: https://doi.org/10.1002/qj.4691